# Analytical and Experimental Verification of Seepage Irrigation using Arduino Microcontroller

Faridoun A.M. Allawi
Retired Professor
Water Resources Engineering, College of Engineering,
Baghdad University, Baghdad, 100071, Iraq

## ABSTRACT
Electrical analog simulation of the subirrigation process inside a classroom is a task that no researcher has ever performed. Therefore, the purpose of this research is to design an experimental setup within the classroom to create an electrical analog of the linearized transient partial differential equation describing subirrigation (seepage irrigation). An **RC** analog circuit controlled by an Arduino microcontroller, linked to software LabVIEW, is used to achieve this purpose. The analytically derived Fourier series solution of the linearized transient partial differential equation governing subirrigation is verified experimentally against the solution of Kirchhoff's partial differential equation, which describes the unsteady current flow through the constructed **RC** circuit. The physical parameters (transmissivity and evapotranspiration rate) of the linearized equation are simulated as constants in the constructed **RC** analog. The agreement between the calculated and observed isochrones of the rising water table levels of the subirrigation process is excellent, indicating that both Fourier solutions are physically and mathematically identical. The constructed electrical analog demonstrates a pedagogical use for the versatile Arduino microcontroller. The power of analogs should form an integrated part of learning groundwater physics.

## Keywords
LabVIEW, Arduino, Transient Subirrigation, Kirchhoff's Law, RC

## 1. INTRODUCTION

Subirrigation is a method of delivering water to plants from below the root zone. It is a practice that controls the water table at specific levels by raising or lowering it. This technique involves artificially adding water to the soil profile underground to moisten the crop root zone for a set period. Essentially, it is a water management method and is the reverse process of drainage. Systems can be designed to operate in either steady-state or transient modes. In a transient mode, water is pumped into the drains and kept at a relatively high level until the water table reaches the root zone. Then, the irrigation water supply is turned off, allowing the water table to be lowered by evapotranspiration. The constant "water level" subirrigation (seepage) technique used in this research differs from controlled injection subirrigation or saturation subirrigation. While controlled drainage and subirrigation are important water management strategies in many regions, the specific conditions under which this technique can most effectively increase crop yield are not fully understood. According to Nelson, K. et al. [1], ideal areas for subirrigation are those with: (1) high soil hydraulic conductivity, enabling water to move quickly from drain tiles into the soil; (2) an impermeable layer in the soil, which allows water to be raised to a desired depth; and (3) flat land topography. In subirrigation designs, high evapotranspiration requires a "high-water table demand," which necessitates large water storage capacity and more frequent replenishment to prevent plant drying. Engineers must accurately estimate evapotranspiration based on canopy, climate, and soil conditions to determine proper irrigation schedules. Monitoring evapotranspiration helps prevent overwatering and maintain optimal soil moisture, ensuring system efficiency and water conservation. In arid regions facing severe water shortages, understanding the relationship between irrigation and evapotranspiration is crucial for future water resource management. Evapotranspiration (**ET**) is modeled using an electrical analogy by treating water vapor flux as an electrical current, with resistance factors such as aerodynamic and canopy resistance represented as electrical resistors. The Penman-Monteith (P-M) and Shuttleworth-Wallace (S-W) models use this analogy, with the S-W model extending the P-M approach by including separate resistances for soil evaporation and plant transpiration, thereby enabling it to model **ET** from heterogeneous surfaces.

Subsurface water movement in hydrological or engineering systems can be analyzed using analogs, as described by Bouwer [2]. These analogs directly simulate the transmission and storage properties of soil, which are relevant parameters in water movement processes. Principles and techniques for constructing and operating analogs include calculating resistance and capacitance values for network analogs, simulating fixed, free, and infinite boundaries, including unsaturated flow, solving quasi-steady flow problems, analyzing diffusion-type flow systems, simulating horizontal and vertical flow systems, instrumentation, and data conversion. Direct electric analogs are relatively simple to build and operate, enabling solutions for flow systems that are not suitable for mathematical analysis. However, there is a limit to the complexity of flow systems that analogs can handle, and at some point, digital computers become more appropriate.

Allawi [3] described an experimental verification of the analytically derived Fourier solutions for the land drainage case (water table drawdown) using an Arduino microcontroller connected with LabVIEW software. The experimental results showed full agreement with the analytical solutions. Incorporating technology into education offers effective opportunities, especially in STEM fields (Science, Technology, Engineering, and Mathematics). In this context, the Arduino platform is a low-cost, easy-to-use microcontroller ideal for physics teaching. According to Atkin [4], different but related models can illustrate the essential physics of one-dimensional heat flow. The first model is a step-by-step process using SMATH Studio, while the second involves an electric **RC** ladder connected to an Arduino microcontroller. Comparing both approaches highlights the power of analogies in learning physics. Coban and Erol [5] conducted a study to examine how Arduino–based STEM education affects the cognitive levels in mechanics and scientific creativity, focusing on topics like vectors, kinematics, dynamics, and work-energy. Coban and

Erol's research is significant because it explores how Arduino use impacts learning outcomes in physics courses taken by preservice teachers at the university level.

The fact that the differential equations describing groundwater flow, electricity, and heat flow are all identical has more than just academic importance, Domenico [6]. For similar initial and boundary conditions, a solution to one of these equations applies to all of them. The hydrologic equivalents of the relevant physical parameters and boundary conditions still need to be identified for a hydrologic solution. Textbooks on electricity and heat flow have greatly contributed to the theories of groundwater flow. Experiments demonstrating a one-to-one correspondence between equations describing hydrologic, thermal, and electrical phenomena—such as the Laplace equation, diffusion equation, and wave equation—serve as effective physical models. When it's possible to find an analogy between two phenomena, one of them becomes easier to observe; information from the simpler phenomenon can then inform us about the other, Domenico [6]. In applying transient flow to drains, it's important to compare theory with model data. One application of heat flow in drainage theories is the method introduced by Glover (Schilfgaarde [7]). Glover derived an equation from the heat flow equation that relates the spacing of tile drains to the rate at which the water table drops at a specific height above the drains. It's important to remember that the solution to Glover's differential equation depends on the analytical solution of the one-dimensional heat equation. The finite difference model developed by Tang and Skaggs [8] is used to solve the nonlinear Boussinesq equation with boundary conditions for drainage and subirrigation. In a large laboratory soil tank, Tang and Skaggs [8] compared their solutions with experimental results. The soil water characteristic and hydraulic conductivity functions were measured using standard methods and used as inputs in the numerical solution to the Boussinesq equation. Although the predicted water table drawdown was somewhat slower than observed, the overall agreement between the numerical solutions and the experimental data was generally good.

To date, no researcher has undertaken an electrical analog simulation of the subirrigation process within a classroom setting. This research addresses that gap by designing an electrical analog—specifically, an **RC** circuit controlled by an Arduino microcontroller and interfaced with LabVIEW software—to model the linearized transient partial differential equation governing subirrigation (seepage irrigation). The study experimentally verifies the analytically derived Fourier series solution of Kirchhoff's partial differential equation through this classroom-based analog simulation. This innovative approach is the first of its kind, as prior research has not employed it to validate the analytical solution for subirrigation. Key physical parameters, such as transmissivity and evapotranspiration rate, are treated as constants in the constructed **RC** analog. By leveraging the versatility of Arduino, this research not only advances the study of subirrigation but also demonstrates the powerful pedagogical value of analog models in groundwater physics education.

The remaining sections of this research study are as follows: Section 2 provides an analytical solution to the linearized Boussinesq partial differential equation, which describes the rise of the water table in transient subirrigation influenced by evapotranspiration. Section 3 explains an analog simulation of the Boussinesq equation using Kirchhoff's transient current partial differential equation. Section 4 explains LabVIEW computer programming. Section 5 presents the results of this study's work example and includes an in-depth discussion supported by graphs. Section 6 shares the conclusions derived from this research, and Section 7 discusses limitations and future directions.

## 2. MATHEMATICAL MODELING

By considering the water table movement (**h**) to be small compared with the water-bearing stratum's average water table height ($\hat{\mathbf{h}}$), and considering evapotranspiration to take place, the following Boussinesq equation:

$$\mathbf{K}\frac{\partial}{\partial \mathbf{x}}\left[\hat{\mathrm{h}} + (\mathbf{h} - \hat{\mathrm{h}})\right]\frac{\partial \mathbf{h}}{\partial \mathbf{x}} + \mathbf{e} = \mathbf{f}\frac{\partial \mathbf{h}}{\partial \mathbf{t}} \qquad (\mathbf{1})$$

Becomes after linearization as:

$$\mathbf{K}\hat{\mathrm{h}}\frac{\partial^2 \mathbf{h}}{\partial \mathbf{x}^2} + \mathbf{e} = \mathbf{f}\frac{\partial \mathbf{h}}{\partial \mathbf{t}} \qquad (\mathbf{2})$$

Where, referring to Figure 1, $\mathbf{h = h\,(x, t)}$ is the distance of the water table above the impermeable layer (reference plane), (**t**) is time, (**f**) is the drainable or (fillable) porosity (storage coefficient), (**e**) is the rate of water lost by evapotranspiration (**e** is negative), and ($\mathbf{K}\,\hat{\mathbf{h}}$) is the aquifer transmissivity. Introducing the non-dimensional parameters, $\boldsymbol{\tau} = \mathbf{[(K\,\hat{h}\,t)/(fL^2)]}$, and $\boldsymbol{\xi} = \mathbf{(x/L)}$, equation (2) may be written as:

$$\frac{\partial^2 \mathbf{h}}{\partial \boldsymbol{\xi}^2} + \boldsymbol{\mu} = \frac{\partial \mathbf{h}}{\partial \boldsymbol{\tau}} \qquad (\mathbf{3})$$

Where $\boldsymbol{\mu} = \mathbf{[(eL^2)/(K\,\hat{h})]}$, and the average depth of flow $\hat{\mathbf{h}} = \mathbf{(d + h2/2)}$. (**d**) and (**h2**) are defined in Figure 1. The boundary and initial conditions measured from the reference plane of Figure 1 are:

**B.C.1** $\mathbf{h = ho,\ \xi = 0,\ \tau > 0,}$

**B.C.2** $\mathbf{h = ho,\ \xi = 1,\ \tau > 0,}$

**I.C.** $\mathbf{h\,(\xi, 0) = h1,\ 0 \le \xi \le 1,\ \tau = 0.}$

The Fourier series solution of equation (3) is:

$$\mathbf{h}(\boldsymbol{\xi}, \boldsymbol{\tau}) = -\boldsymbol{\mu}\frac{\boldsymbol{\xi}^2}{\mathbf{2}} + \boldsymbol{\mu}\frac{\boldsymbol{\xi}}{\mathbf{2}} + \mathbf{ho} + \frac{\mathbf{4}}{\boldsymbol{\pi}}\sum_{\mathbf{n=0}}^{\infty}\frac{\mathbf{1}}{(\mathbf{2}\boldsymbol{n} + \mathbf{1})}\left(\boldsymbol{\mu}\frac{\boldsymbol{\xi}^2}{\mathbf{2}} - \boldsymbol{\mu}\frac{\boldsymbol{\xi}}{\mathbf{2}} - \mathbf{ho} + \mathbf{h1}\right)\mathbf{sin}(\mathbf{2}\boldsymbol{n} + \mathbf{1})\boldsymbol{\pi}\,\boldsymbol{\xi}\,\mathbf{e}^{-(\mathbf{2n+1})^2\boldsymbol{\pi}^2\boldsymbol{\tau}} \qquad (\mathbf{4})$$

If the evapotranspiration source (**e**) of equation (1) is (**0**), then $\boldsymbol{\mu} = \mathbf{0}$, and equation (4) reduces to,

$$\mathbf{h}(\boldsymbol{\xi}, \boldsymbol{\tau}) = \mathbf{ho} - \frac{\mathbf{4(ho - h1)}}{\boldsymbol{\pi}}\sum_{\mathbf{n=0}}^{\infty}\frac{\mathbf{1}}{(\mathbf{2n} + \mathbf{1})}\,\mathbf{e}^{-(\mathbf{2n+1})^2\boldsymbol{\pi}^2\boldsymbol{\tau}}\,\mathbf{sin}(\mathbf{2}\boldsymbol{n} + \mathbf{1})\boldsymbol{\pi}\,\boldsymbol{\xi} \qquad (\mathbf{5})$$

The mathematical details of the solution of equation (3) are given in Appendix A.

The mathematical difference between equations (4) and (5) clarifies the role of the parameter (**e**), the evapotranspiration rate. Clearly, with the absence of (**e**), the values of $\mathbf{h}\,(\boldsymbol{\xi}, \boldsymbol{\tau})$ of equation (5) for a given initial water table height (**ho**) and given aquifer transmissivity ($\mathbf{K}\,\hat{\mathbf{h}}$) and storage coefficient (**f**) would be higher than those calculated by equation (4).

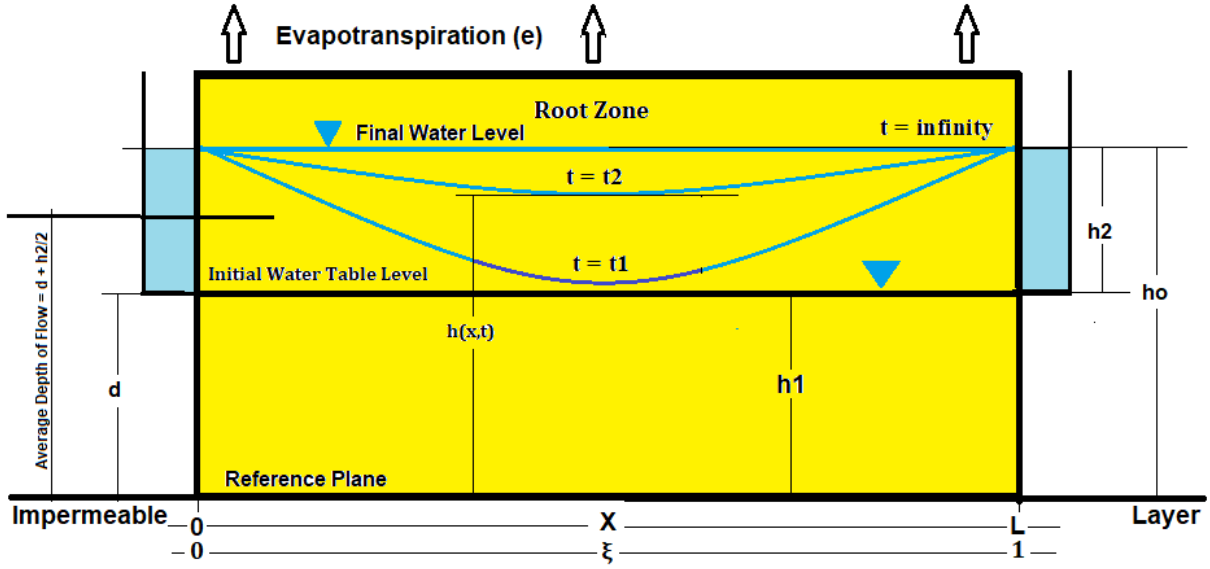


**Fig. 1 Typical 1D cross-section of a subirrigation system**

Skaggs [9, 10] have used numerical methods to solve the nonlinear Boussinesq equation (1) subject to subirrigation conditions for both initially horizontal and initially draining profiles. Equation (1) is written numerically in a finite difference form and solved on a digital computer. The non-dimensional graphical plots of (**h/ho**) values vs. (**τ**) are for a point midway between the drains (**ξ = x/L = 0.5**). The plots are for a given range of (**h1/ho**) values. Figures of the graphical solution have shown that for (**τ**) values ≥ (1) and (**μ**) values greater than (-3), the values of the steady-state solution of the ratio (**h/ho**) are lower than those of (**μ = 0**).

## 3. ANALOG SIMULATION

Many hydrological factors influence groundwater flow, including boundary conditions, irrigation seepage, anisotropic soil materials, and fluctuating infiltration, making solutions complex, lengthy, and sometimes impractical. Therefore, simulating an aquifer with a model becomes necessary. Analog models allow studying aquifer responses through actual measurements with different inputs. These models physically replicate field conditions using real aquifer materials. The **RC** network is based on the analogy between Darcy's law and Ohm's law, involving a resistor-capacitor mesh. Currents that represent evapotranspiration rates are applied at the mesh's nodal points based on the evapotranspiration value (**e**). Evapotranspiration (**e**) is modeled using an electrical analogy by treating water vapor flux as an electrical current, while resistances that oppose this flux—such as aerodynamic and canopy resistance—are represented as electrical resistors. The Penman-Monteith (P-M) and Shuttleworth-Wallace (S-W) models utilize this analogy, with the S-W model extending the P-M approach by adding separate resistances for soil evaporation and plant transpiration, allowing it to model **ET** from heterogeneous surfaces. Figure 2a shows a breadboard setup of a typical differential element of an RC circuit for the subirrigation case affected by evapotranspiration (**e**). The **RC** circuit components are defined as follows: resistive (**R**) components in Figure 2a simulate the hydraulic conductivity (**K**) of the aquifer; the capacitor (**C**) represents the storage coefficient (**f**); and the current supplied by the **LM334z** element with its (**RSET**) component models the evapotranspiration rate (**e**). Figure 2b represents a vector diagram of the input and output currents of the differential element of Figure 2a. The current analysis for the differential element of Figure 2b is:

$$\mathbf{i1 = i2 + i3 + i4\Delta xe} \qquad (6)$$

Or, $\mathbf{i1 - i2 = i3 + i4\Delta xe}$

Knowing that: $\mathbf{i1 - i2 = -\frac{\partial i}{\partial xe}\,\Delta xe}$

According to Ohm's law, the current $\mathbf{i = -\frac{1}{R}\frac{\partial V}{\partial xe}}$ , therefore,

$$\mathbf{-\frac{\partial i}{\partial xe}\,\Delta xe = \frac{\partial}{\partial xe}\left(\frac{1}{R}\frac{\partial V}{\partial xe}\right)\Delta xe = \frac{1}{R}\frac{\partial^2 V}{\partial xe^2}\,\Delta xe}$$

$$\mathbf{i3 = C\,\Delta xe\frac{\partial V}{\partial te}}$$

**i4** = Constant current source equivalent to the evapotranspiration rate (**e**) of equation (2).

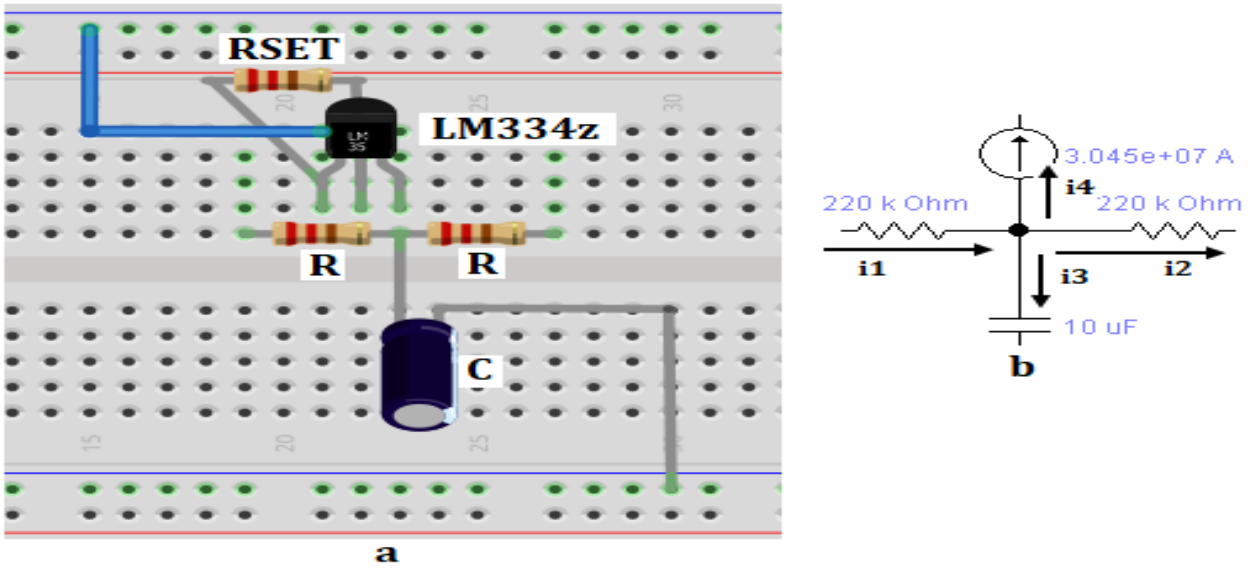


**Fig. 2 Breadboard attachment of typical differential element components of the RC circuit (a) and its current vector diagram (b)**

After some mathematical manipulation, the following partial differential equation is obtained:

$$\frac{\partial^2 V}{\partial xe^2} = RC\left(\frac{\partial V}{\partial te}\right) + RI \qquad (7)$$

Where **I** = **i4** (the constant current source**) is** to be fed at each differential element of the **RC** network. It is to be noticed that the current source (**I**) of equation (7) simulates the evapotranspiration parameter (**e**) of equation (2). Introducing the non-dimensional parameters, **δ = [te/(m²RC)],** and **β = (xe / m)**, equation (7) may be written as:

$$\frac{\partial^2 V}{\partial \beta^2} = \frac{\partial V}{\partial \delta} + q \qquad (8)$$

where $q = m^2RI$ . The parameter (**m**) is defined as the number of differential elements comprising the **RC** analog of Figure 3. The boundary and initial conditions of equation (8) of the subirrigation case are:

**B.C.1 V = Vo, β = 0, δ > 0,**

**B.C.2 V = Vo, β = 1, δ > 0,**

**I.C. V = 0, 0 ≤ β ≤ 1, δ = 0.**

**V** = nodal voltage, **Vo** is the Arduino—Atmega (**5**) volts power source, **R** = resistance value, **C** = capacitor value, **I** = constant current source, **xe** = flow direction, and **te** = analog time in seconds.

It is worth noting that the non-dimensional form of equations (3) and (8) allows for a reduction in the number of experiments needed to analyze the influence of each physical parameter and to derive scaling laws necessary for conducting cost-effective, small-scale experiments. Resistors act as energy dissipaters, similar to transmissivity (**T**), while capacitors serve as potential energy containers, akin to the storage coefficient (**f**), Agarwal [11]. Each resistor in an **RC** network corresponds to the reciprocal of the aquifer's transmissivity, and each capacitor is comparable to the aquifer's storage parameter. The resistance to fluid flow decreases as the aquifer thickness (**d**) increases, while the storage capacity increases proportionally with thickness. It is helpful to express equation (8) using the non-dimensional variables shown in Figure 3. The upward arrows in Figure 3 indicate the constant current (**I**) in each differential element.

The Fourier series solution of equation (8) is:

$$V(\beta,\delta) = \left(\frac{q}{2}\beta^2 - \frac{q}{2}\beta + Vo\right) + \frac{4}{\pi}\sum_{n=0}^{\infty}\frac{1}{(2n+1)}\left(-\frac{q}{2}\beta^2 + \frac{q}{2}\beta - Vo\right)\sin((2n+1)\pi\beta)e^{-(2n+1)^2\pi^2\delta} \qquad (9)$$

The mathematical details of the solution of equation (8) are given in Appendix B.

Figure 4 shows the Breadboard circuit diagram of a resistance-capacitance network designed by software Fritzing to simulate the virtual transient subirrigation flow system of Figure 1 influenced by evapotranspiration (**e**). The Figure shows the detailed connections of all the electrical units used in the design and construction of the **RC** network, including the Arduino Mega microcontroller, which acts as a data acquisition instrument.

It is to be noticed that all the capacitors of the analog of Figure 4 are initially discharged which means that **V (β, 0)** equals **(0)** and for similarity purposes, the initial condition of the function **h (ξ, 0)** (which is the initial water level elevation at (**t** = **0**) of Figure 1 must be (**0**); therefore, (**h1**) value of equation (4) equals (**0**).

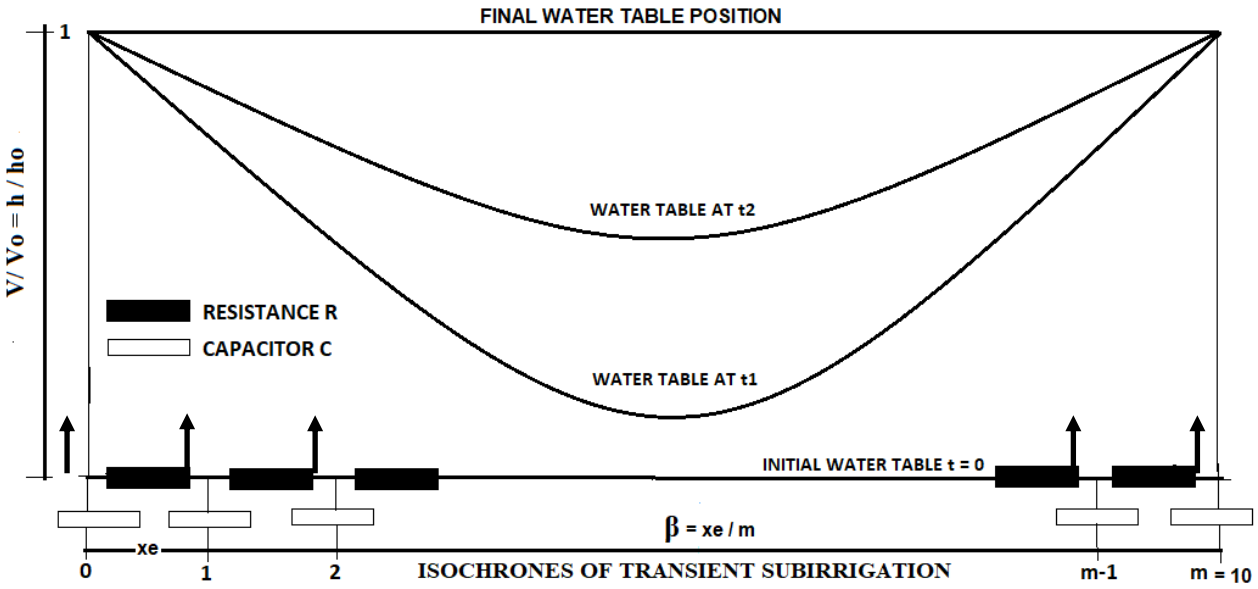


**Fig. 3 Non-dimensional axes definitions of the RC analog of the transient subirrigation case**

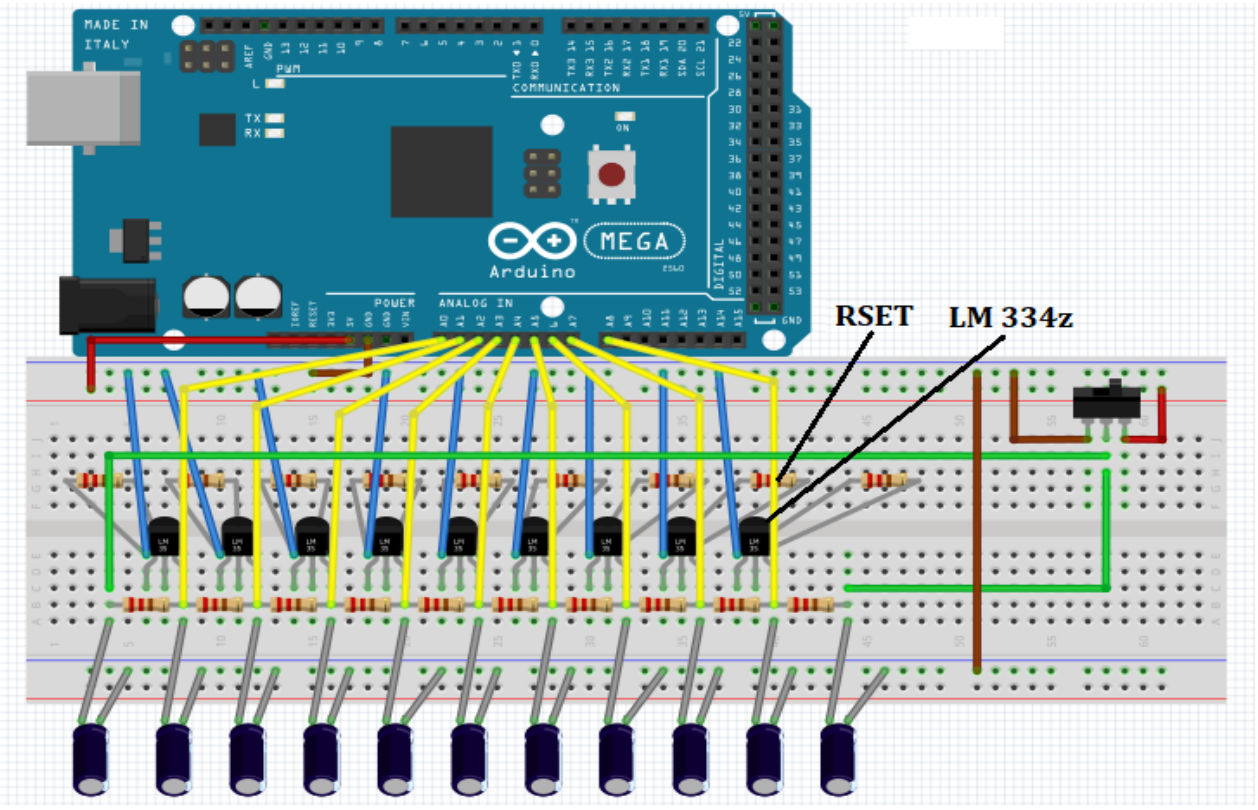


**Fig. 4 Fritzing Breadboard circuit design of the electrical analog of a virtual 1D transient subirrigation system influenced by evapotranspiration**

The network resistors and capacitors selected for simulating the hydrologic case studies are 220000 Ohms and 10E-6 Microfarads, respectively. The network consists of 10 segments, each equal to (L/m) units long. At the boundaries, capacitors with half the values, i.e., 5E-6 Microfarads, are used, following Rushton and Redshaw [12]. In this study, different soil hydraulic conductivity (**K**) and storage coefficient (**f**) values can be simulated in the analog by adjusting resistance (**R**) and capacitance (**C**) values. This allows the analog to model anisotropic soil conditions easily. The **LM334z** component and the **RSET** in Figures 2 and 4 simulate the physical evapotranspiration component (e) of the model shown in Figure 1 and provide the necessary constant-current source for each differential element of the **RC** network. With an **RSET** value of 220000 Ohms, the **LM334z** unit in Arduino supplies a steady current (**I**) of 3.04545E-7 Amperes. Different crop evapotranspiration rates (**e**) can be easily modeled by selecting appropriate **RSET** values for the **LM334z** component. Based on the chosen **R**, **C**, and **I** values of the hydrologic flow system, the properties of the simulated case are **ho** = 5 m, **h2** = 1 m, **h1** = 0 m, **d** = 4 m, and **K** = 0.0325 m/hr. **L** = 25 m, **f** = 0.05, and **t** = 90.0676 hours.

## 4. COMPUTER PROGRAMMING

Figure 5a shows the object-oriented block diagram of the ANALOG SIMULATION LabVIEW Tab Control for the RC network. The LINX Firmware Wizard from the Maker Hub add-on allows the Arduino microcontroller to connect to the PC via LabVIEW. Text files are used to transfer data into and out of LabVIEW, and these files can be opened in spreadsheet programs like Excel. Writing data to a spreadsheet file is the method used to transfer LabVIEW data into a spreadsheet. The timed loop structure in Figure 5a runs one or more subprograms or frames sequentially, with each iteration executing at the specified period. During each iteration, the Analog Read.vi and the Write Delimited Spreadsheet.vi are run. The Analog Read.vi reads the values from the specified analog input channels of the Arduino microcontroller. The Write Delimited Spreadsheet.vi converts a 2D array of double-precision numbers into a text string and writes or appends this string to an existing file. The Timed Loop Structure is executed sequentially by the LINX Open.vi device in the Maker Hub software. The LabVIEW Write Delimited Spreadsheet.vi function allows LabVIEW to function as a data acquisition system for measuring (**V/Vo**).

The object-oriented block diagram of the experimental subirrigation LabVIEW Tab Control is shown in Figure 5b. The case structure within the block diagram plots the isochrones of the measured (**V/Vo**) values against those calculated by equation (9). The LabVIEW Formula control icon, as shown in Figure 5b, computes equation (9), and the LabVIEW Waveform Graph indicator visually plots both values. The Waveform Graph displays the array data it receives as inputs (Data Acquisition Device).

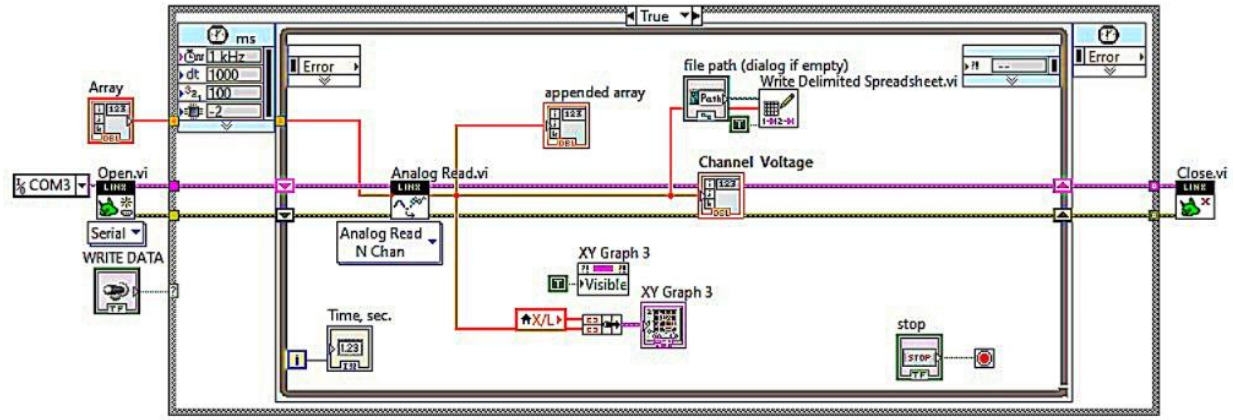


**Fig. 5a Block diagram of the ANALOG SIMULATION LabVIEW Tab control of the RC analog**

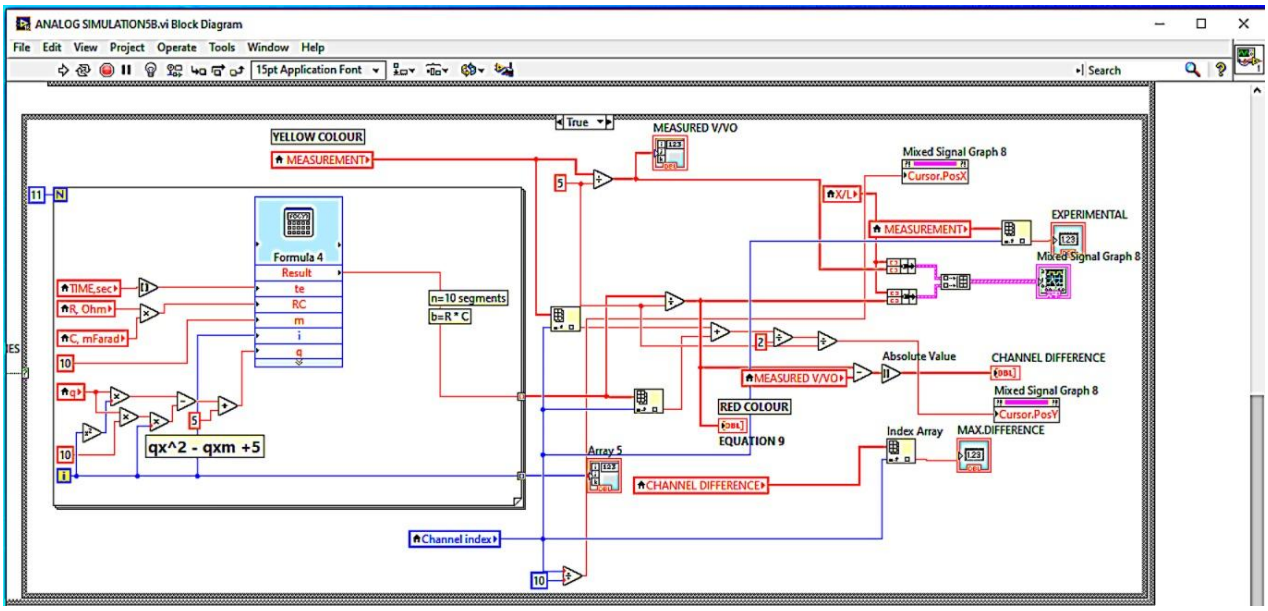


**Fig. 5b Block diagram of the EXPERIMENTAL SUBIRRIGATION LabVIEW Tab control of the RC analog**

The LabVIEW block diagram of the statistical analysis is shown in Figure 5c. The case structure of this block diagram includes a LabVIEW Waveform Graph indicator for plotting the differences between the measured (experimentally) and the calculated values of the derived Kirchhoff's equation (9) of each Arduino analog channel, as well as the statistical LabVIEW VIs for calculating the mean square error and the Standard Deviation of the datasets of the experimental and analytical results. The LabVIEW **MSE** VI takes, for any given channel or port at any given time (**t**), two input arrays: the observed (measured **V/Vo**) and the calculated values of equation (9) (as shown in the Figure), which are used to compute the average squared difference between them. The LabVIEW numerical operators, the **MEASURED SD**, and the

**CALCULATED SD of EQ. 9** output the values of the Standard Deviation of the experimental dataset results and those of the analytical solution of equation (9), respectively.

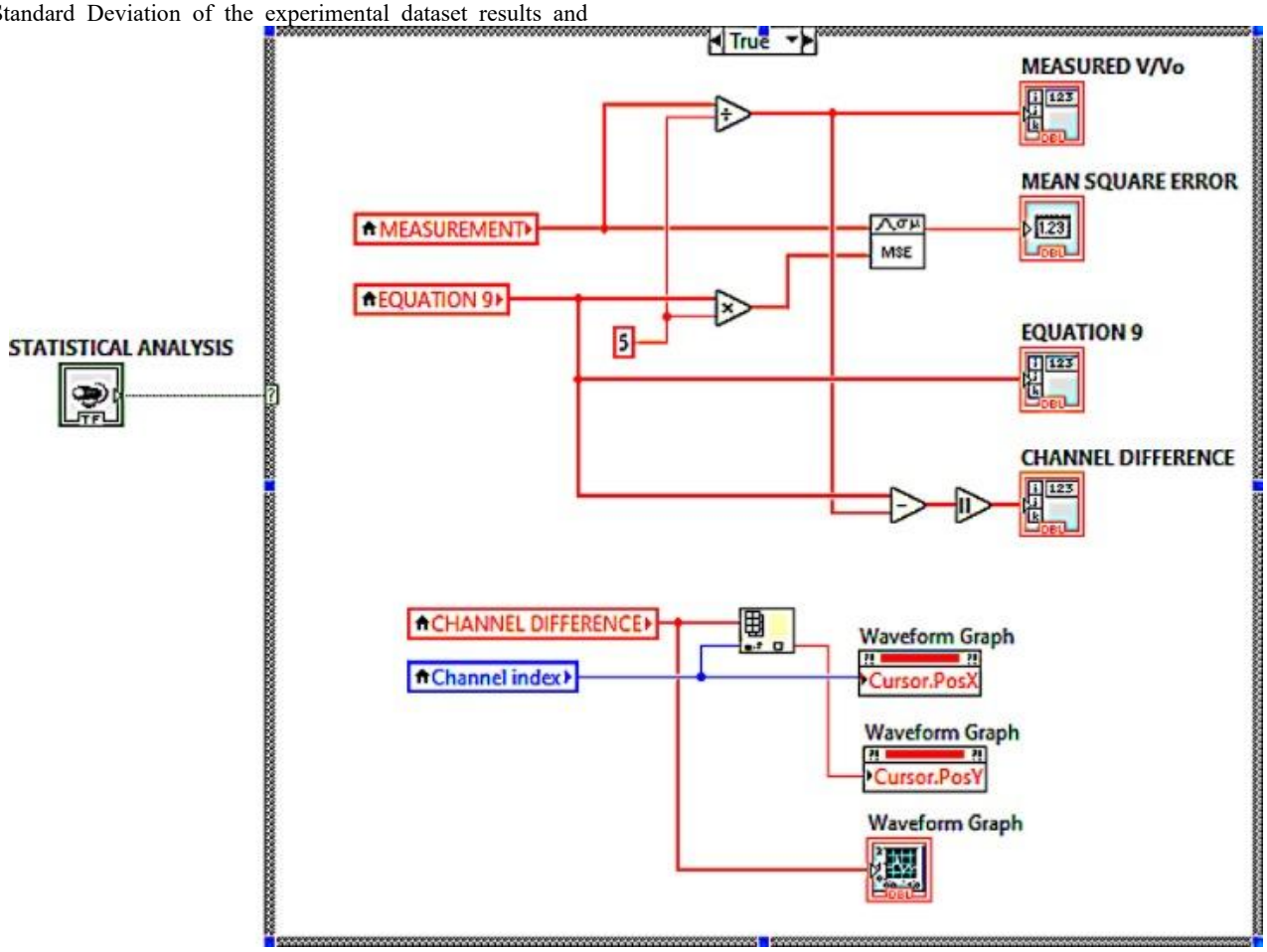


**Fig. 5c LabVIEW block diagram of the statistical analysis**

The isochrones of equations (4) and (9) plotted by the LabVIEW Mixed Single Graph control of the case structure of the LabVIEW TAB control are shown in Figure 5d. The icon of the LabVIEW Formula control, shown in Figure 5d, calculates the value of (**h/ho**) in equation (4).

The Analog Simulation of the LabVIEW TAB - control of the graphic display of Figure 6 shows graphically the experimental output of the nodal voltage readings of the analog differential elements of the **RC** network at an analog time **te** = 153 seconds. The Figure clearly shows the steady-state elliptical distribution of the variable (**V**) of equation (9) along the non-dimensional horizontal axis (**β** = **xe/m**) of the constructed analog.

## 5. RESULTS AND DISCUSSION

The subirrigation method used in this study is the constant water- level type. By blocking the drainage pipes, a fixed water level (ho) in the topsoil is maintained, ensuring a sufficient water table to promote capillary rise to the plant root zone. The technique of subirrigation used in this research differs from that of saturation subirrigation and controlled injection subirrigation. Mathematically, the following example will demonstrate the application and validity of this method.

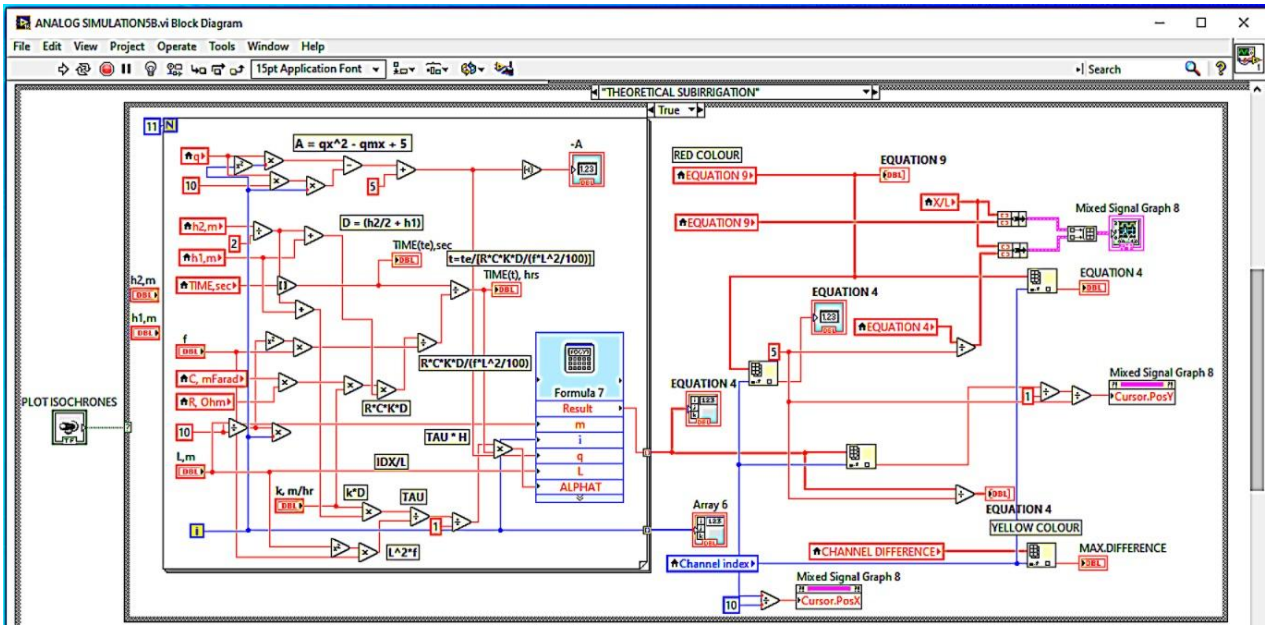


**Fig. 5d LabVIEW Block diagram of the THEORETICAL SUBIRRIGATION Tab control of the RC analog**

**Application 5.1:** The hydrological properties of a subirrigation project are: **ho** = 5 m, **h1** = 0 m, **h2** = 1 m, **d** = 4 m, **K** = 0.0325 m/ hr.., **L** = 25 m, **f** = 0.05, **t** = 97.12509713 hrs., and **e** = 0.00156779 m/hr. Use:

**1-** Equation (9), to calculate at **β** = 1/2, the (**V/Vo**) value, knowing that (**Vo**) = 5 volts, **m** = 10, **R** = 220E3 Ohm, and **RSET** = 220 Ohm.

**2-** Equation (4), to calculate at **ξ** = 1/2, the (**h/ho**) value.

**3-** Use the LabVIEW program to plot the statistical Arduino channel differences and their **MSE** value. Also, calculate the Standard Deviation values of the experimental and analytical datasets. Discuss the results.

**4-** Using the LabVIEW program and the **RC** network, plot and compare the measured (**V/Vo**) results against those of equation (9). Use the calculated analog time (**te**).

**5-** Use the LabVIEW program to plot graphically the results of equations (4) and (9) for the calculated analog time (**te**). Discuss the graphical results.

**6-** For the given data**,** use the numerical Figures of the solution of the non-linearized Boussinesq equation derived by Skaggs [14] and [18] to calculate the ratio of (**h/ ho**).

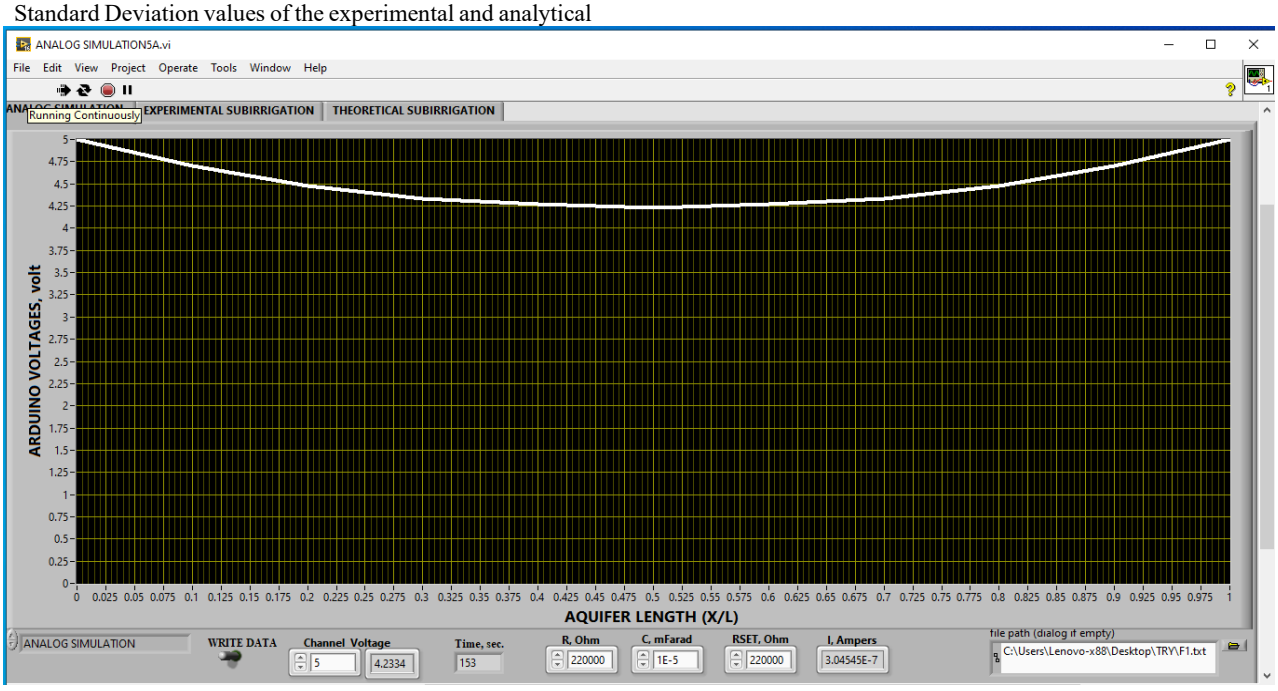


**Fig. 6 Analog results of subirrigation influenced by aquifer properties and evapotranspiration**

**Solution**

Check the following calculations:

Due to the similarity of equations (3) and (8, (**-μ = q** ), the value of the source current **I** can be calculated as:

$$\mathbf{I} = \frac{\mathbf{e} * \mathbf{L}^2}{\mathbf{m}^2 * \mathbf{R} * \mathbf{K} * \hat{\mathbf{h}}} = \frac{\mathbf{0.00156779} * \mathbf{625}}{\mathbf{100} * \mathbf{220E3} * \mathbf{0.0325} * (\mathbf{4} + \mathbf{0.5})} = \mathbf{3.04545\ E-7ampere}$$

$$\mathbf{q} = \mathbf{m^2RI} = \mathbf{100} * \mathbf{220E3} * \mathbf{3.04545E-7} = \mathbf{6.6999\ volt}$$

$$\boldsymbol{\mu} = \frac{\mathbf{e} * \mathbf{L}^2}{\mathbf{K} * \bar{\mathbf{h}}} = \frac{\mathbf{-1.56779\ E-3} * \mathbf{625}}{\mathbf{0.0325} * (\mathbf{4} + \mathbf{0.5})} = -\mathbf{6.6999\ \ meter, (e) is\ negative; upward\ flow}$$

$$\mathbf{te} = \frac{\mathbf{R} * \mathbf{C} * \mathbf{K} * \hat{\mathbf{h}} * \mathbf{t}}{\Delta\mathbf{X}^2 * \mathbf{f}} = \frac{\mathbf{220E3} * \mathbf{10E-6} * \mathbf{0.0325} * (\mathbf{4} + \mathbf{0.5}) * \mathbf{97.12509}}{\left(\frac{\mathbf{25}}{\mathbf{10}}\right)\mathbf{\hat{}2} * \mathbf{0.05}} = \mathbf{100\ s}$$

$$\boldsymbol{\tau} = \frac{\mathbf{K} * \hat{\mathbf{h}} * \mathbf{t}}{\mathbf{f} * \mathbf{L\hat{}2}} = \frac{\mathbf{0.0325} * (\mathbf{4} + \mathbf{0.5}) * \mathbf{90.0676}}{\mathbf{0.05} * \mathbf{25}^2} = \mathbf{0.4545}$$

$$\boldsymbol{\delta} = \frac{\mathbf{te}}{\mathbf{m}^2 * \mathbf{R} * \mathbf{C}} = \frac{\mathbf{100}}{\mathbf{100} * \mathbf{220E3} * \mathbf{10\ E-6}} = \mathbf{0.4545}$$

**1**- From equation (9), **V** = **4.10280 volts**, and (**V/Vo**) = **0.82056**.

2- From equation (4), **h** = **4.10280 meters** above the reference level, and (**h/ho**) = **0.82056**

**3-** Refer to Figure 7.

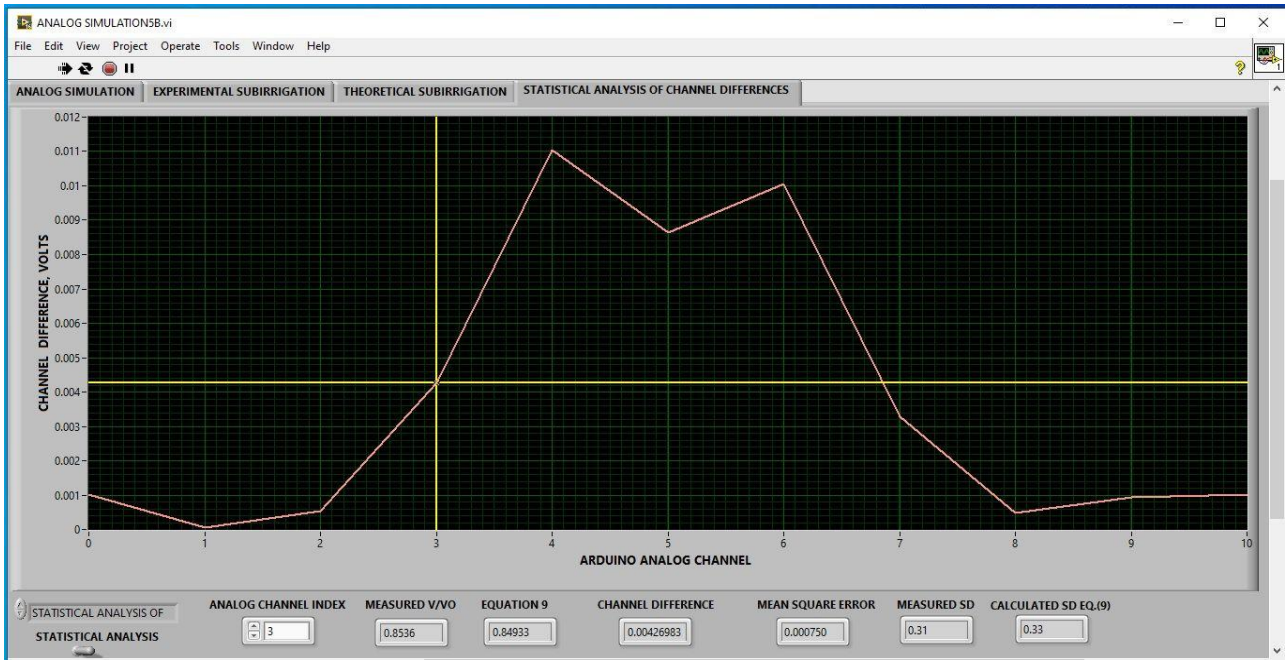


**Fig.7 LabVIEW statistical analysis**

Figure 7 shows the graphical display of the differences, the mean square error (**MSE**), and the standard deviation values of the measured voltages of the analog differential elements (**V/Vo**) and those calculated from the Fourier series solution of Kirchhoff's transient current partial differential equation (9). An excellent agreement exists between the measured values of (**V/Vo**) and those calculated by the Fourier sine series equation (9), as indicated by the Standard Deviation values of the results. The results indicate the exactness and correctness of the derived Fourier series solution of equation (9).

**4**- The right screen in Figure 8 shows the graphical variation of the nodal voltage readings (**V**) of the **RC** analog differential elements and those calculated by equation (9). The channel difference between both dataset values (the measured and the calculated) is (**0.00863**) volts. The left LabVIEW graphic display in Figure 8 shows the increase in nodal voltages of the recharging capacitors of the differential elements that compose the **RC** network in the transient subirrigation case of this research study.

**5-** Refer to Figure 9. The curves of equations (4) and (9) of Figure 9 showed complete similarity in form and magnitudes.

**6**- The non-dimensional numerical Figures of the non-linearized Boussinesq solution require calculating the following non-linearized parameters:

$$\boldsymbol{\mu} = \frac{-\mathbf{e} * \mathbf{L\hat{}2}}{\mathbf{K} * \mathbf{ho\hat{}2}} = -\mathbf{1.207615}, \boldsymbol{\tau} = \frac{\mathbf{K} * \mathbf{t} * \mathbf{ho}}{\mathbf{f} * \mathbf{L}^2} = \mathbf{0.46834}\ \text{and,}\ \mathbf{D} = \frac{\mathbf{h1}}{\mathbf{ho}} = \mathbf{0}$$

Insertion of the values of these parameters in the numerical Figures of [**u** = -1] and [**u** = -2] gives, after interpolation, a (**h/ho**) value of (**0.8**).

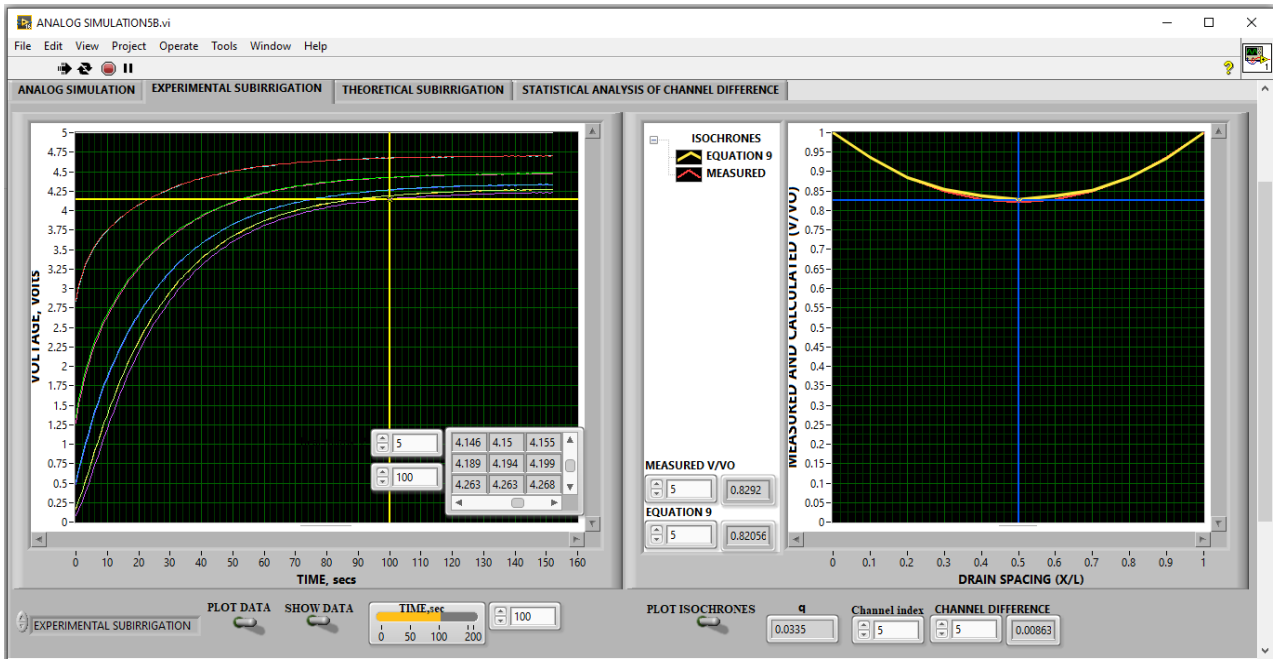


**Fig. 8 Measured and calculated values of V/Vo of the transient subirrigation case (right) and the voltage increase with time (te) across the network capacitors (left)**

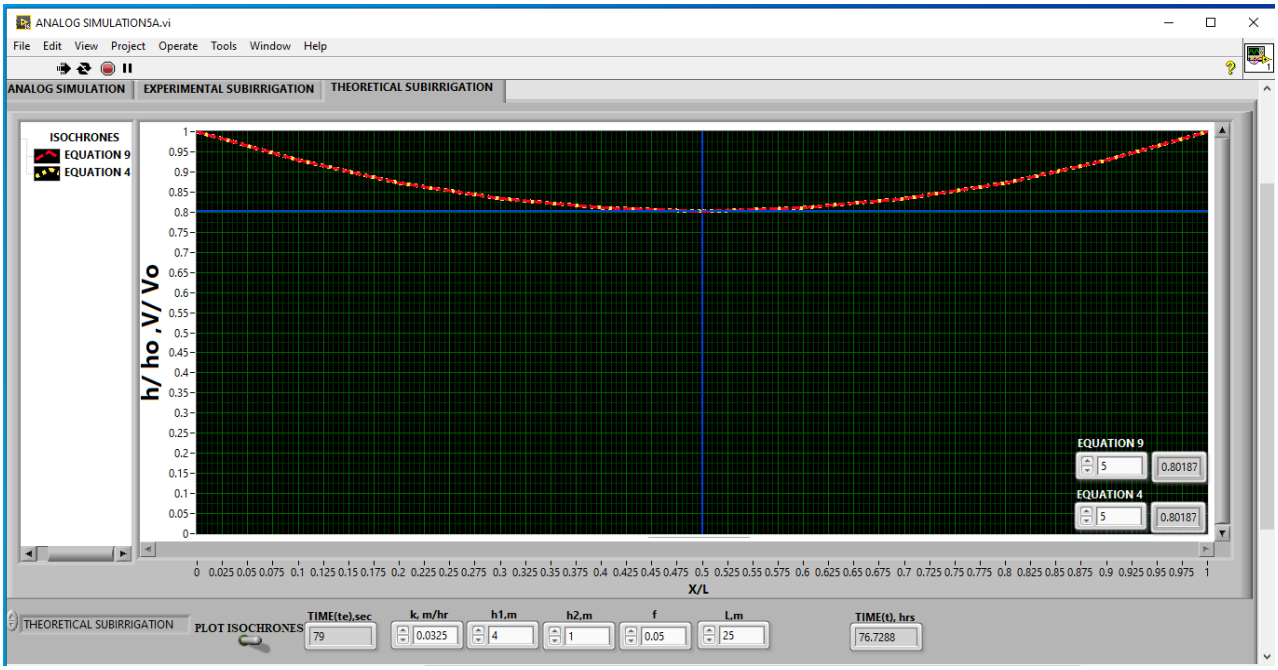


**Fig. 9. LabVIEW graphical display of equations (4) and (9)**

The worked example has indicated the following:

(a) The limiting factor in designing a subirrigation system is the time (**t**) required to raise the water table to supply crop evapotranspiration (**e**) demands. Considering this aspect is necessary for the successful OPERATIONS of subirrigation systems under transient conditions.

(b) The Fourier series solution of the derived Kirchhoff's partial differential equation is found to be highly accurate, as indicated by the standard deviations of the calculated and measured values of (**V/Vo**).

(c) The approximation (**ĥ**) used for linearizing the Boussinesq equation proved to be experimentally accurate and exact. Regardless of whether the researcher is dealing with the flow of groundwater, electricity, or heat, the differential equation describing each is similar in form and principle; only the physical parameters of the equations are named differently. Generally, this research indicated an excellent agreement in trend and accuracy between the derived experimental solution of the partial differential equation (9) of the transient electrical flow of the **RC** network and the derived theoretical analytic solution of the partial differential equation (4) of the transient subirrigation case under the influence of the aquifer parameters (**K**) (**d**), (**f**), (**ho**), and (**e**).

(d) The LabVIEW graphical plot of the differences between the measured (**V/Vo**) and those calculated from the Fourier series of equation (9) varied with the analog channels (differential elements) of the **RC** circuit and were extremely minimal (check the standard deviation values of both in Figure 8). The minimal losses are due to the increasing leakage currents of the model capacitors over time; the tolerances of the capacitors and resistors in the **RC** network, which did not significantly influence the results presented in this research. The minimal losses of the **RC** analog are quantified by the calculated differences between the measured (**V/Vo**) values and those calculated by the Fourier series solution of equation (9).

(e) The LabVIEW graphic plot in Figure 9 shows that equations (4) and (9) are physically and mathematically similar in form and yield identical results. That is true since the exponential functions of both equations depend on the same physical properties of the soil.

# 6. CONCLUSIONS

This research revealed the following:

1- The rationale for using an **RC** network inside the classroom is its compactness, simplicity, and effectiveness in teaching the simulation of soil physical and mechanical properties and related physical parameters imposed on the soil system, such as evapotranspiration rates. The constructed electrical analog demonstrates a pedagogical use for the versatile Arduino microcontroller. The power of analogs should form an integrated part of learning groundwater physics.

2- Differential equations describing groundwater flow are identical in form and principle to those governing electricity and heat flow. For a given set of analogous boundary conditions, a solution to one of these equations applies to all of them. The experimental results shown in Figure 8 of the RC network are accurate and closely match the analytical solution of the partial differential equation describing Kirchhoff's law for transient electrical flow through the **RC** network. The maximum difference between the measured and calculated values of (**V/Vo**) is indicated as (0.00863), with an **M.S.E**. of 0.000750. Despite tolerance errors in the resistors and capacitors, and increasing leakage currents in the model capacitors over time, the isochrones of the solutions of equations (4) and (9) in Figure 9 show excellent agreement in trend, accuracy, and physical and mathematical similarity, because the exponential functions of both equations depend on the same physical properties of the soil.

3- The analytical and experimental results of the linearized Boussinesq partial differential equation (1) used in this research, if compared with those of the numerical solution of the non-linearized form of the Boussinesq partial differential equation, agree favorably well.

4- Graphically, the Figures of this research study indicate that for the cases of ($\boldsymbol{\mu} \neq 0$), the calculated and measured values of the subirrigation ratios (**h/ho**) and (**V/Vo**) of equations (4) and (9) are always less than those of ($\boldsymbol{\mu} = 0$) due to the influence of the physical parameter (**e**) of evapotranspiration.

5- Subirrigation controls water management by actively raising and lowering the water table within the soil through a system of subsurface pipes (drains), pumps, and control structures, ensuring water availability for crops and evapotranspiration.

# 7 LIMITATIONS and FUTURE WORK

The only limitation of the physical model described by equation (4) in this research is that all the parameters of the partial differential equation are constants. For future work, the author proposes the following studies:

1- The influence of variable aquifer transmissivity (**K $\hat{\mathbf{h}}$**), variable storage coefficient (**f**), and variable initial water table height (**ho**) on the rate of rise of the water table under constant evapotranspiration rate (**e**) (constant current source in the analog) can be easily incorporated by selecting suitable values of (**R**), (**C**), and (**Vo**).

2- By selecting different current source values (**I**), the influence of the spatial variation of the evapotranspiration rate (**e(x)**) on the rate of rise of the water table under constant, aquifer transmissivity, and (**ho**) parameters can be easily incorporated in the analog.

To establish a one–to–one correspondence between the electric and hydrologic systems (the aquifer and its analog), it is necessary to introduce scale factors or factors of proportionality, which are given in Appendix B. However, from a hydrological perspective, equation (4) is simulated accurately in the **RC** analog, and the simulation results confirm this.

# 8 DECLARATIONS

*8.1 Conflict of Interest***:**

The corresponding author states that there is no conflict of interest.

*8.2 Author's Contribution:*

The author confirms sole responsibility for the following: study conception and design, data collection, analysis and interpretation of results, and manuscript preparation.

*8.3 Funding:*

There is no funding for the publication of this research study.

*8.4 Acknowledgement:*

The author deeply appreciates the anonymous reviewers for their fruitful and constructive suggestions that helped further improve this paper.

*8.5 Data Availability Statement:*

Using the constructed analog of this paper can create all the data supporting this research's findings.

*8.6 Using AI Tools:*

The author declares that no AI tool was used in this research paper.

# 9 REFERENCES

[1] Nelson, K., Kjaersgaard, J., Reinhart, B., Frankenberger, J., Wilson, R., Gunn, K., Lee, C., Abendroth, L., Bowling, L., and Niaghi, A.R., Corn Yield Response to Drainage Water Recycling using Subirrigation, https://www.extension.purdue.edu/extmedia/ABE/ABE-163-W.pdf, 2021

[2] Bouwer, H., Analyzing Subsurface Flow with Electric Analogs, Water Resources Research, Vol. (3), Issue (3), 1967

[3] Allawi, F.A.M., Experimental Verification of the Transient

Land Drainage Equation using LabVIEW-Arduino Atmega Microcontroller, International Journal of Mathematics and Computer in Engineering, 4(1) 15–24, 2026

[4] Atkin, K., 1D heat Flow Simulations using Simple Digital and Analog Models, Physics Education, vol. (56), no. (3), P 1-7, 2021

[5] Coban, A. and Erol, M., Impact of Arduino-Based STEM Education on the Cognitive Domain Level of Machines and Scientific Creativity. LUMAT. International Journal on Mathematics, Science, and Technology https://doi.org/10.31129/LUMAT.12.4.2231 Education. 12(4), 16.

[6] Domenico, P., Concepts and Models in Groundwater Hydrology, McGraw-Hill, New York, 1972

[7] Schilfgaarde, J.V., Drainage for Agriculture, American Soc. of Agronomy, Inc., Publisher, Wisconsin, 1974

[8] Tang, Y. K. and Skaggs, R., Experimental evaluation of theoretical solutions for subsurface drainage and irrigation, Water Resources Research v. (13), issue (6), pp: 957 – 965, 1977

[9] Skaggs, R.W., Water table movement during subirrigation. Transactions ASAE 16: 988 - 993, 1973

[10] Skaggs, R.W., Water movement factors important to the design and operation of subirrigation systems. Transactions ASAE 24: 1553 - 1561, 1981

[11] Agarwal, V.C., Groundwater Hydrology, PHI, New Delhi, 2012.

[12] Rushton K.R. and Redshaw S.C., Seepage and Groundwater Flow Numerical Analysis by Analog and Digital Methods, John Wiley & Sons, New York, 1979

[13] Carslaw, H.S. and Jaeger, J.C., Conduction of Heat in Solids. Oxford University Press, Oxford, 1959

# APPENDIX

## Appendix A

Equation (3) is a non-homogeneous partial differential equation that can be reduced to a steady state and a transient state where the ends are kept initially at (**h**) values equal to (**ho**) (**0 ≤ ξ ≤ 1),** Carslaw and Jaeger [13]. Put: **h (ξ, τ) = u(ξ) + w (ξ, τ),** where **u(ξ)** and **w (ξ, τ) (**the steady and the transient state functions) satisfy the following equations:

$$\frac{\partial^2 u}{\partial \xi^2} = -\mu \qquad (A1)$$

**u = ho** at (**ξ = 0)** and (**ξ = 1),** and

$$\frac{\partial^2 w}{\partial \xi^2} = \frac{\partial w}{\partial \tau} \qquad (A2)$$

**w = 0**, (**0 ≤ ξ ≤ 1). A**t (**τ = 0), w (ξ, 0) = h (ξ, 0) – u(ξ).** Initially, at (**τ = 0**), **h (ξ, 0) = h1** above the reference plane of Figure 1.

Whatever the initial value of **h (ξ, 0), t**he steady state solution of equation (**A1**) for an initially horizontal water table of Figure 1 is:

$$u(\xi) = -\mu\frac{\xi^2}{2} + \mu\frac{\xi}{2} + ho.$$

In the separation of variables, the solution of equation (**A2**) would be:

$$w(\xi,\tau) = \sum_{n=1}^{\infty} bn\, \sin(n\pi\xi) e^{-n\hat{}2\pi\hat{}2\tau}.$$

where $bn = 2\int_{\xi=0}^{\xi=1} w(\xi,0)\sin(n\pi\xi)\, d\xi$.

Initially $w(\xi, 0) = h(\xi, 0) - u(\xi) = h1 - (-\mu\frac{\xi\hat{}2}{2} + \mu\frac{\xi}{2} + ho) = \mu\frac{\xi^2}{2} - \mu\frac{\xi}{2} - ho + h1.$ Therefore, substitution and integration yield: $bn = \frac{4}{n\pi}(\mu\frac{\xi^2}{2} - \mu\frac{\xi}{2} - ho + h1)$ **n = 1, 3, 5….**

Thus

$$h(\xi,\tau) = -\mu\frac{\xi^2}{2} + \mu\frac{\xi}{2} + ho + \frac{4}{\pi}\sum_{n=0}^{\omega}\frac{1}{(2n+1)}\left(\mu\frac{\xi^2}{2} - \mu\frac{\xi}{2} - ho + h1\right)\sin(2n+1)\pi\xi e^{-(2n+1)^2\pi^2\tau} \qquad (A3)$$

If the evapotranspiration source (**e**) of equation (1) is (**0**), then **μ = 0,** and equation (**A3**) reduces to,

$$h(\xi,\tau) = ho - \frac{4(ho-h1)}{\pi}\sum_{n=0}^{\infty}\frac{1}{(2n+1)}\, e^{-(2n+1)^2\pi^2\tau}\sin(2n+1)\pi\xi \qquad (A4)$$

## Appendix B

Equation (8) is a non-homogeneous partial differential equation that can be reduced to a steady-state voltage solution and a transient voltage solution, where the ends are kept at zero volts [16]. Put **V (β, δ) = G(β) + F (β, δ)**, where **(G)** and **(F)** are functions satisfying the following differential equations:

$$\frac{\partial^2 G}{\partial \beta^2} = q \qquad (B1)$$

**G = Vo** at (**β = 0**) and (**β = 1**), and

$$\frac{\partial^2 F}{\partial \beta^2} = \tau e\, \frac{\partial F}{\partial \delta}. \qquad (B2)$$

where **τe = RC.** With the following boundary and initial conditions:

**B.C.1 F = 0, β = 0, δ > 0,**

**B.C.2 F = 0, β = 1, δ > 0,**

**I.C. V (β, 0) = 0, (0 ≤ β ≤ 1). A**t (**δ = 0), F (β, 0) = V (β, 0) – G(β).** Initially, at (**δ = 0**). Initially, **V (β, 0) = 0.** The steady state solution of equation (**B1**) is:

$G = \frac{q}{2}\beta^2 - \frac{q}{2}\beta + Vo.$ And, by the separation of variables, the solution of equation (**B2**) would be as follows:

$$F(\beta,\delta) = \sum_{n=1}^{\infty} an\, \sin(n\pi\beta) e^{-n\hat{}2\pi\hat{}2\delta}.$$

where $an = 2\int_0^1 F(\beta,0)\sin(n\pi\beta)\, d\beta.$

**F (β, 0) = V (β, 0) – G(β) = 0 – (**$\frac{q}{2}\beta^2 - \frac{q}{2}\beta + Vo$**). P**erforming the integration above gives the value of (**an**): $an = \frac{4}{n\pi}(-\frac{q}{2}\beta^2 + \frac{q}{2}\beta - Vo)$**,** therefore

$$\mathbf{V}(\boldsymbol{\beta}, \boldsymbol{\delta}) = (\frac{\mathbf{q}}{\mathbf{2}}\boldsymbol{\beta}^{\mathbf{2}} - \frac{\mathbf{q}}{\mathbf{2}}\boldsymbol{\beta} + \mathbf{Vo}) + \frac{\mathbf{4}}{\boldsymbol{\pi}} \sum_{\mathbf{n=0}}^{\infty} \frac{\mathbf{1}}{(\mathbf{2n+1})} \left(-\frac{\mathbf{q}}{\mathbf{2}}\boldsymbol{\beta}^{\mathbf{2}} + \frac{\mathbf{q}}{\mathbf{2}}\boldsymbol{\beta} - \mathbf{Vo}\right) \mathbf{sin}\,((\mathbf{2n} + \mathbf{1})\boldsymbol{\pi\beta})\mathbf{e}^{-(2n+1)^2\pi^2\delta} \quad (\mathbf{B3})$$

To establish a one–to–one correspondence between the electric and hydrologic systems, it is necessary to introduce scale factors or factors of proportionality. The following one-to-one relationship is defined by Rushton and Redshaw [12]:

Let the relationship between the electrical potential (**Vo**) and the groundwater potential (**ho**) be:

$$\mathbf{Vo} = \mathbf{F1} * \mathbf{ho} \quad (\mathbf{B4})$$

Where **F1** is a convenient scaling factor.

Let the electrical resistance (**R**) be proportional to the distance between the nodal points ($\Delta\mathbf{x}$) and inversely proportional to the transmissivity ($\mathbf{K}\hat{\mathbf{h}}$)

$$\mathbf{R} = \frac{\mathbf{F2} * \Delta\mathbf{x}}{\mathbf{K}\hat{\mathbf{h}}} \quad (\mathbf{B5})$$

**F2** is a convenient scaling factor that relates the electrical resistance to the aquifer transmissivity.

The third independent relationship that can be defined between the electrical capacitance (**C**) and the storage coefficient (**S**) of the aquifer is:

$$\mathbf{C} = \Delta\mathbf{X} * \mathbf{f} * \mathbf{F3} \quad (\mathbf{B6})$$

Where **F3** is a convenient scaling factor between both parameters.

From these three independent relationships, the following relationship between the analog time (**te**) of the **RC** network and the physical time (**t**) of the hydrological model can be derived:

$$\mathbf{te} = \mathbf{F2} * \mathbf{F3} * \mathbf{t} \quad (\mathbf{B7})$$

$$\mathbf{F2} = \frac{\mathbf{R} * \mathbf{K}\hat{\mathbf{h}}}{\Delta\mathbf{x}} \quad (\mathbf{B8})$$

$$\mathbf{F3} = \frac{\mathbf{C}}{\Delta\mathbf{x} * \mathbf{f}} \quad (\mathbf{B9})$$

Substitution of equations (**B8**) and (**B9**) into equation (**B7**) gives,

$$\mathbf{t} = \frac{\Delta\mathbf{x}^{\mathbf{2}} * \mathbf{f} * \mathbf{te}}{\mathbf{R} * \mathbf{C} * \mathbf{K}\hat{\mathbf{h}}} \quad (\mathbf{B10})$$